Poster
#
179

Contact information:
Valentina Vongrad
University Hospital Zurich
Rämistrasse 100, 8091 Zurich
Switzerland
Valentina.vongrad@usz.ch
+41442559238

The Role of RNA Interference in HIV-1 Infected Primary Human Monocyte-Derived Macrophages

Vongrad V[1*], Imig J[2*], Mohammadi P[3*], Kishore S[4], Jaskiewicz L[4], Zavolan M[4], Hall J[2], Beerenwinkel N[3], Günthard HF[1] and Metzner KJ[1]

[1] University Hospital Zurich, Department of Medicine, Division of Infectious Diseases and Hospital Epidemiology, Zurich, Switzerland, [2] Institute of Pharmaceutical Sciences, ETH Zurich, Switzerland

*[3] Department of Biosystems Science and Engineering, ETH Zurich Basel, Switzerland [4] Computational and Systems Biology, University of Basel, Switzerland *Contributed equally to this work*

Background

Micro RNAs (miRNAs) and other small noncoding RNAs (sncRNAs) are key players in post-transcriptional gene regulation. We and other groups have described the presence of HIV-1 derived sncRNAs in different experimental setups; however, their biological function has remained so far to a large extent unknown. Here we used a global, comprehensive approach to investigate whether viral small RNAs play a role in the RNA interference (RNAi) pathway in primary human monocyte-derived macrophages (MDMs). Specifically, we aimed to characterize small RNA profiles of the host and HIV-1 and their possible impact on the viral life cycle.

Methods

Primary human monocytes from healthy blood donors were isolated and differentiated into macrophages in the presence of 10% human serum and M-CSF. We applied Argonaute 2 (Ago2) photoactivatable ribonucleoside-enhanced crosslinking and immunoprecipitation (PAR-CLIP) to MDMs infected with HIV-1_{JRFL} (MOI 0.1) for 14 days from two different donors. It has been previously demonstrated that this approach enables identification of Ago2-bound miRNAs as well as of the miRNA-targeted mRNAs. Illumina sequencing was performed on PAR-CLIP and small RNA (18 to 30 nt) samples from the same donors, and small RNA sequencing was performed on HIV-1 infected MDMs from two additional donors.

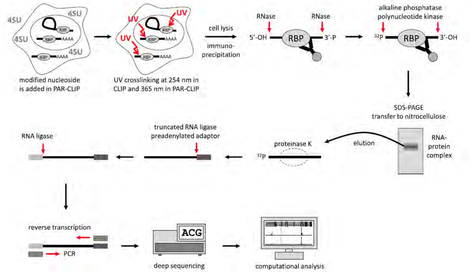


Figure 1. Illustration of PAR-CLIP. Incubation with a photoactivatable nucleoside analog 4SU is performed in PAR-CLIP and cells are crosslinked with 365 nm UV light. After immunoprecipitation, radioactively labeled RNA–protein complexes are resolved by SDS–PAGE and blotted to nitrocellulose membrane. After adaptor ligation and reverse transcription, a pilot PCR determines the number of cycles chosen to allow library amplification with minimal PCR amplification bias (adapted from Jaskiewicz *et al*, 2012).

Results

PAR-CLIP reveals the absence of HIV-1 sncRNAs in Ago2-RISC in HIV-1 infected MDM

- Over 33.8 million reads could be aligned to either the human or the HIV-$1_{JR\text{-}FL}$ genome (**Table 1**), identifying different RNA species (**Figure 2**).

	HIV-$1_{JR\text{-}FL}$	Output reads	Reads aligned
Donor 2	no	31,073,335	12,379,701 (39.84%)
Donor 4	no	13,595,536	8,587,138 (63.16%)
Donor 2	yes	16,822,014	5,909,192 (35.13%)
Donor 4	yes	12,470,608	6,971,961 (55.91%)

Table 1: High-throughput sequencing of RNA libraries derived by Ago2 PAR-CLIP of MDM, HIV-$1_{JR\text{-}FL}$ infected (n=2) and non-infected (n=2). Output reads represent reads after size selection (≥13 nts) and removal of adaptor-adaptor sequences.

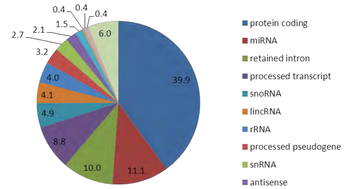


Figure 2. RNA species present in all PAR-CLIP samples (n=4) in %.

- 5 hits in total mapped to HIV-$1_{JR\text{-}FL}$ with indicative T-to-C (thymidine to cytidine transition) PAR-CLIP mutations to exclude sequences derived by nonspecific binding (**Table 2A and B**).
- 3 out of 5 clusters derived from HIV-1 infected samples (**Table 2A and B**).
- 1st read cluster mapped to HIV-$1_{JR\text{-}FL}$ at position 637 in antisense orientation representing $tRNA^{Lys}$ matching the primer binding site (PBS) of HIV-1, present in both, infected and non-infected MDM (**Table 2A and B**).
- 2nd read cluster resembled the corresponding sense strand (HIV-$1_{JR\text{-}FL}$ position 636) lacking diagnostic mutations was found twelve times (**Table 2B**).
- 3rd read cluster mapped to the viral genome at nucleotide position 801 in antisense orientation, but was also present in non-infected MDM (**Table 2A and B**).

A. Non-infected MDM (n=2)

Start position HIV-$1_{JR\text{-}FL}$	Strand	Length (nt)	Coverage	Total Ts	Total T-to-Cs
636	Sense	19	0	0	0
637	Antisense	24	1700	6046	31
801	Antisense	17	3	10	1
1614	Sense	23	18	90	0
5910	Antisense	19	13	39	0
8025	Sense	48	24	194	0

B. HIV-$1_{JR\text{-}FL}$ infected MDM (n=2)

Start position HIV-$1_{JR\text{-}FL}$	Strand	Length (nt)	Coverage	Total Ts	Total T-to-Cs
636	Sense	19	12	12	0
637	Antisense	24	477	1712	14
801	Antisense	17	27	104	23
1614	Sense	23	0	0	0
5910	Antisense	19	0	0	0
8025	Sense	48	0	0	0

Table 2: Localization and characteristics of HIV-1 encoded sncRNAs identified by AGO-2 PAR-CLIP. Shown are the cluster loci according to HIV-$1_{JR\text{-}FL}$, strand orientation, length of the indicated sequence, coverage total number of Ts in the indicated sequences, and the number of diagnostic T-to-C mutations.

Small RNA sequencing confirms the presence of HIV-1 sncRNAs in the whole cell lysate in MDM

- Different RNA species were recovered from small RNA fraction in 4 donors. HIV-$1_{JR\text{-}FL}$ infected MDM harbored ~1.2% HIV-1 reads of the small RNA fraction, while non-infected MDM remained negative for HIV-1 sncRNAs (**Figure 3A and B)**
- HIV-1 read clusters were distributed all over the genome, most clusters derived from sense orientation, while minor sequences originated from antisense orientation and were largely represented by $tRNA^{Lys}$ (**Figure 4**).
- Most cellular miRNAs expression levels were not significantly altered by HIV-1 infection. However, 16 miRNAs were significantly upregulated and 3 downregulated (**Figure 5**).

	HIV-$1_{JR\text{-}FL}$	Output reads	Reads aligned
Donor 1	no	17,635,535	14,547,394 (82.49%)
Donor 2	no	27,114,541	22,029,614 (81.25%)
Donor 3	no	21,175,108	17,481,336 (82.56%)
Donor 4	no	37,839,512	31,678,367 (83.72%)
Donor 1	yes	21,255,845	17,163,001 (80.74%)
Donor 2	yes	17,913,668	14,335,116 (80.02%)
Donor 3	yes	27,440,998	20,601,911 (75.08%)
Donor 4	yes	16,347,062	12,988,200 (79.45%)

Table 3: High-throughput sequencing of small RNA libraries of MDM, HIV-$1_{JR\text{-}FL}$ infected (n=4) and non-infected (n=4). Output reads represent reads after size selection (≥13 nts) and removal of adaptor-adaptor sequences. Reads aligned represent the read number aligned to either the human or the HIV-$1_{JR\text{-}FL}$ genome.

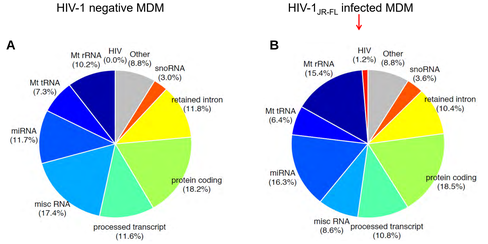


Figure 3. Frequencies of RNA species assessed by small RNA deep-sequencing excluding rRNA.
(**A**) RNA species detected in non-infected MDM (4 donors). (**B**) RNA species detected in MDM (4 donors) infected with HIV-$1_{JR\text{-}FL}$ for 14 days.

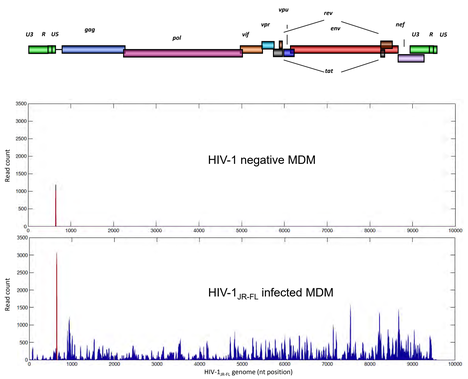


Figure 4. HIV-1 read density coverage in small RNA sequencing mapping to HIV-1 genome. An average of all HIV-1 negative (n=4, middle panel) over HIV-1 positive (n=4, lower panel) libraries are shown. Highlighted in red is $tRNA^{Lys}$ mapping in antisense orientation to HIV-1. Upper panel show a schematic sketch of the HIV-1 genomic organization.

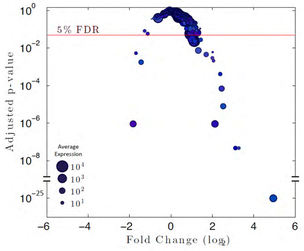


Figure 5. Differential miRNA expression in HIV-$1_{JR\text{-}FL}$ infected (n=4) versus non-infected (n=4) MDM. The size of circles is proportional to their average expression level in logarithmic scale. The X-axis represents fold change in log2 scale, the Y-axis represents adjusted p-values in log10 scale. The red line sets the threshold for 5% false discovery rate (FDR).

Conclusion

Our data indicate that it is unlikely that HIV-1 sncRNAs are incorporated as functional miRNAs or resemble targets for host miRNAs in Ago2-RISC in MDM. However, the presence of HIV-1 sncRNA as detected by small RNA sequencing implies alternative functional roles or biogenesis pathways. Future efforts are needed to uncover potential functions of HIV-1 derived sncRNAs in MDMs or other HIV-1 host cell types.

Acknowledgements

This study was supported by the Swiss National Science Foundation grant No. 31003A-112670